Modeling the Interaction of the Phosphate Group in Nucleotides with Copper(I) in the Gas Phase: Reactivity of Cu$^+$ with Orthophosphoric Acid and Its Monomethyl Ester

A. Luna, S. Gevrey, and J. Tortajada*

Laboratoire de Chimie Organique Structurale, Universite Pierre et Marie Curie, CNRS UMR 8587, 4 Place Jussieu, Boîte 45, 75252 Paris Cedex 05, France

Received: March 26, 1999; In Final Form: October 15, 1999

The gas-phase reactivity of orthophosphoric acid $(HO)_3P{=}O$ with the cation Cu$^+$ has been investigated through the use of mass spectrometry experiments and DFT calculations. Its monomethylated ester $(CH_3O)(HO)_2P{=}O$ has been also theoretically studied at the same level in order to take into account the possible effects of methylation. Computational results, including structural features, vibrational frequencies, and binding energies, obtained with the hybrid three-parameter B3LYP density functional combined with relativistic ECPs and associated valence basis set, were reported. Final binding energies have been evaluated using extended basis sets. Additional calculations performed with several "all electron" basis sets are also included for comparison. For some of the minima of the $[Cu,H_3PO_4]^+$ hypersurface, the nature of the different Cu−O bonds as well as the character of the orbitals involved were analyzed by means of the Bader topological analysis and NBO method.

Introduction

Over the past years, the study of gas-phase organometallic ion chemistry has experienced a rapid growth.[1] With the aim of determining relevant thermodynamical data such as gas-phase binding energies or enthalpies of formation, a wide variety of experimental techniques were employed.[2] Moreover, the help of theoretical studies has allowed real progress concerning the understanding of the main features that can result from the interaction between a metallic ion with organic compounds. The combined experimental and theoretical approaches on isolated species also allow a better knowledge of intrinsic interactions from effects due to solvation and/or solvent-induced phenomena. Then, obtaining accurate data on the complex issue from the interaction of metallic cations with simple ligands and determining the level of theory required to accurately model these complexes are the first steps toward developing reliable models of the interaction between metallic cations and more complex molecules.[3]

In this field of investigations, mass spectrometry has proved to be a good experimental tool to investigate the gas-phase intrinsic reactivity of transition metal monocations with different neutral systems of biological relevance. The formation and the specific fragmentations of cation-bound biomolecules is a promising alternative to obtain structural information with essentially analytical goals, such as peptide sequencing for example. Thus, understanding the details of (i) local interactions, (ii) fragmentation mechanisms, and (iii) associated energetics of metal ion−neutral reactions are matters of high interest.

In recent years, our group has been interested in the study of these kinds of reactions. In particular, we have studied the gas-phase reactions between Cu$^+$ and guanidine,[4] formamide,[5−7] and urea.[8] These small molecules can be used as model systems to understand the behavior of more complicated systems of biological relevance such as amino acids, peptides, and nucleobases as long as they contain the mentioned functional groups. Regarding the Cu$^+$, it is well-known that copper is one of the most important transition metals involved in biochemical

processes, thus a considerable effort has been devoted recently to investigate the interactions between Cu$^+$ and α-amino acids.[9] The interaction of organic molecules with Cu$^+$ presents some specific and interesting peculiarities; first, the nature of the interaction is likely different from that found for some other alkali metal ions;[4,10] second, it has been shown that the Cu$^+$ binding energies are directly related to the gas-phase basicities.[6,11] Other catalytic effects for some isomerization reactions have been demonstrated in recent works.[6−7]

Besides peptides, the nucleic acids DNA and RNA are of indisputable biological relevance. Mass spectrometry is actually one of the most promising techniques for fast DNA sequencing in the Human Genome Project.[12] The advances in the mass spectrometry of oligonucleotides and DNA have been particularly rapid since the introduction of fast atom bombardment (FAB) and plasma desorption mass spectrometry (PDMS) methods[15] and, more recently, electrospray ionization (ESI)[13] and matrix-assisted laser desorption/ionization (MALDI)[14] techniques, which must be capable of generating ions containing several hundred bases. In these methods, because the nucleotides are dissolved in a matrix, which usually contains alkali metals (Na$^+$, K$^+$) as impurities, we can observe (in the positive mode) the formation of protonated species (MH$^+$) and alkali metal adduct ions: MNa$^+$ and MK$^+$. In these experimental conditions, it is assumed that in nucleotides, the positively charged alkali metal associates rapidly and strongly with the negatively charged oxygen atom of the phosphate group (P−O$^-$). In a second step the protonation of the base is followed by the cleavage of the subsequent N-glycosidic bond and the phosphodiester backbone.[16] This fragmentation, therefore, is the main remaining problem to be solved before the analysis of larger oligonucleotides. To increase the stability of oligonucleotides and avoid the backbone cleavage, some solutions have been used such as chemical modifications of bases[17] or the replacement of alkali ions.[18] Another alternative could be proposed, which consists of using metal transition ions and, more precisely, Cu$^+$ as an ionization agent.

Phosphate Group Interaction with Gas-Phase Cu(I)

J. Phys. Chem. B, Vol. 104, No. 1, 2000 **111**

In the gas phase the situation is quite different: the phosphate residue is not anionic, and therefore different nucleotide−Cu$^+$ adducts can be formed. First, metal ion association (as well as protonation) can compete toward the binding of the phosphate group, the sugar, and the base. Therefore, the resulting complexes could have different structures. According to the specificity of copper monocation, which has the tendency to form particularly stable structures in which Cu$^+$ interacts with several sites, some possible isomeric structures can result from the interaction of Cu$^+$ with the potential sites for binding, i.e., the phosphate oxygen atom (P=O), the oxygen atoms of the sugar, the base ring nitrogens, and the exocyclic keto groups. These kinds of structures are of interest because they can ensure the cohesion of the system in avoiding the base loss and the cleavage of the phosphodiester backbone. Actually, because of the lack of experimental results, these assumptions can only be supported by a theoretical approach. However, as the size of these systems is prohibitive for high-level ab initio calculations, our survey has consisted of studying the Cu$^+$ complexation of the different entities that constitute nucleotides, i.e., the neutral phosphate group, the deoxyribose, and the natural bases. The aim of such studies was 2-fold. We hope first to obtain with good accuracy geometrical and thermodynamics data on separated moieties and second to check a reliable theoretical method to consider the interaction of Cu$^+$ with the entire nucleotide.

The study presented here concerns only the reactivity in the gas phase of Cu$^+$ with the neutral phosphate group. Several reviews have been devoted to the molecular structure and the reactivity of phosphate esters both in solution[19] and in the gas phase. On the contrary, very little is known about the gas-phase reactivity of orthophosphoric acid and only very recently were its experimental and theoretical gas-phase acidity[20] and gas-phase proton affinity[21] reported in the literature.

In this work we present an experimental and a theoretical study of the gas-phase reactivity of Cu$^+$ with orthophosphoric acid and its monomethylated ester. Besides, the presence of several basic centers in (HO)$_3$P=O prompted us to evaluate the binding energies by Cu$^+$ association in order to predict possible thermodynamic competitions between cationization sites of the phosphate group and those of the nucleobase when the nucleotide is involved.

The paper is structured as follows: after the statement of the experimental and theoretical methods used, we will describe the experimental features of the CI-FAB mass spectrum resulting from the reactivity of Cu$^+$ with triethyl phosphate, whose adduct ions decompose to yield the complexes of interest (i.e., orthophosphoric−Cu$^+$). Then the structural bonding and the energetic features of the calculated [(HO)$_3$P=O, Cu$^+$] and [(CH$_3$O)(HO)$_2$P=O, Cu$^+$] complexes will be presented and discussed.

Experimental Section

The ion source spectrum was recorded using a VG analytical ZAB-HSQ mass spectrometer of BEqQ geometry.[22] Complexes were generated in a CI-FAB source. The source was constructed from VG analytical EI/CI and FAB ion source parts with the modifications described by Freas et al.[23] A foil of high-purity copper replaces the conventional FAB probe tip. "Naked" metal ions were so generated by bombardment with fast xenon atoms (Xe gas 7−8 keV kinetic energy, 1−2 mA of emission current in the FAB gun). As stated by Schwarz et al.,[24] we can suppose that due to the relatively high pressure in the ion source (10^{-2}−10^{-3} Pa), efficient collisional cooling of the ions takes place and therefore excited states of the Cu$^+$ ions are assumed to not

participate in the observed reactivity. Triethyl phosphate was introduced via a heated inlet system at 100 °C in a nonheated source.

Computational Details

The theoretical treatment of the different systems included in this work was performed using the B3LYP[25] density functional approach in the Gaussian-94 series of programs.[26] This method has been found to be quite reliable as far as the description of metal cation−neutral complexes is concerned, in particular when Cu$^+$ ions are involved.[27] The B3LYP approach is a hybrid method, which includes the Becke's[25] three parameter nonlocal exchange potential with the nonlocal correlation functional of Lee, Yang, and Parr.[28] Geometry optimizations were performed using the effective core potentials (EPCs) of Hay and Wadt[29] with the valence basis set (8s5p5d)/[3s3p2d] for Cu and the D95 double-ζ basis set[30] for the remaining atoms of the system (H, C, O, P). We term this level of theory B3LYP/LAN2DZ. Frequency calculations have been performed, at the same level, with the double aim to characterize the nature of the minima of the hypersurface and to determine the zero-point energy (ZPE) corrections. The energy of all the species involved has been recalculated using the 6-311+G(2df,-2p) basis set for the H, C, P, O atoms. For the Cu atom the (14s9p5d)/[9s5p3d] Wachters−Hay's basis set[31] supplemented with a set of (1s2p1d) diffuse components and with two sets of 7f-type functions and one set of 10g-type functions as the polarization basis. So, the basis function and contraction (15s11p6d2f1g)/[10s7p4d2f1g] was used. For the sake of simplicity we will denote hereafter this basis set as Basis1. As we will show later, the B3LYP/Basis1//B3LYP/LANL2DZ level of theory proportionates a good compromise between reliability and feasibility. For similar cases of Cu$^+$ complexation[4,5] the basis set superposition error (BSSE) correction has been also estimated. We have observed that the BSEE correction, calculated at the highest level mentioned above, is less than 1 kcal/mol. To test the effects that a more complete basis set would have on the results (relative stability of some minima and binding energy between Cu$^+$ and phosphoric acid), we have performed additional calculations using 6-31G, 6-31G(d), 6-311G(d,p), 6-311G(2d,2p), 6-311G(2df,2p), and 6-311+G-(2df,2p) standard basis sets for H, C, O, and P atoms and similar "all electron" basis sets for Cu (which are described in Table 2).

To obtain deep insight on the bonding characteristics of the different species, as well as the possible bond activations occurring in our neutral systems upon Cu$^+$ complexation, we used the atoms in molecules (AIM) theory of Bader.[33] For this purpose we have reevaluated the electronic density using the 6-311G(d,p) basis set (see Table 2). This density allowed us to locate the bond critical points, i.e., points where the electron density function, $\rho(r)$, is a minimum along the bond path and a maximum in the other two directions. The Laplacian of the density, $\nabla^2\rho(r)$ identifies regions of the space wherein the electronic charge is locally depleted ($\nabla^2\rho(r) > 0$) or built up ($\nabla^2\rho(r) < 0$). The former situation is typically associated with interactions between closed-shell systems (ionic bonds, hydrogen bonds, and van der Waals molecules), while the latter characterizes covalent bonds, where the electron density concentrates in the internuclear region. There are, however, significant exceptions to this general rule, mainly when high electronegative atoms are involved in the bonding. Hence, we have also evaluated the energy density, $H(r)$,[34] which does not present these exceptions. In general, negative values of $H(r)$ are

TABLE 1: Absolute and Relative Energies at the B3LYP/ LANL2DZ (E_1) and B3LYP/Basis 1 (E_2) Levels and Zero Point Energy Corrections at the B3LYP/LANL2DZ Level (Hartrees)[a]

	E_1	E_2[b]	ZPE	ΔE_1	BE (E_1)	ΔE_2	BE (E_2)
PCu1	−505.087342	−2284.577173	0.046967	0.0	62.6	0.0	61.1
PCu2	−505.077201	−2284.540121	0.048066	7.1	55.5	23.9	37.1
PCu4	−505.066060		0.046627	13.1	49.4	-	
P_a + Cu$^+$	−504.986544	−2284.476999	0.045535	62.4		62.0	
P_b + Cu$^+$	−504.986168	−2284.478347	0.045485	62.6		61.1	
MPCu1	−544.389221	−2323.892041	0.075714	0.0	65.7	0.0	63.2
MPCu2	−544.378709	−2323.858696	0.076288	7.0	58.8	21.3	41.9
MPCu3	−544.379205	−2323.855756	0.076548	6.8	58.9	23.3	39.9
MP$_a$ + Cu$^+$	−544.283036	−2323.787695	0.074145	65.6		64.5	
MP$_b$ + Cu	−544.283106	−2323.789883	0.074327	65.7		63.2	
P_a	−309.157342	−644.300305	0.045535	−0.2		0.9	
P_b	−309.156966	−644.301653	0.045485	0.0		0.0	
MP$_a$	−348.453834	−683.611001	0.074145	−0.1		1.3	
MP$_b$	−348.453904	−683.613189	0.074327	0.0		0.0	
Cu$^+$	−195.829202	−1640.176694	0.000000			-	

[a] Relative (ΔE) and binding energies (BE) of the different complexes (kcal/mol) under study. [b] These values correspond to single point calculations over the B3LYP/LANL2DZ optimized geometries

TABLE 2: Basis Functions and Contractions for Cu, Depending on the Different Denoted Basis Sets Used

| basis set	Cu
6-31G	(22s16p4d)/[5s4d2d][a]
6-31G(d)	(22s16p4d1f)/[5s4d2d1f][a]
6-311G(d,p)	(14s9p5d1f)/[9s5p3d1f][b]
6-311G(2d,2p)	(14s9p5d2f)/[9s5p3d2f]
6-311G(2df,2p)	(14s9p5d2f1g)/[9s5p3d2f1g]
6-311+G(2df,2p) (Base1)	(15s11p6d2f1g)/[10s7p4d2f1g]

[a] Reference 32. [b] Reference 31.
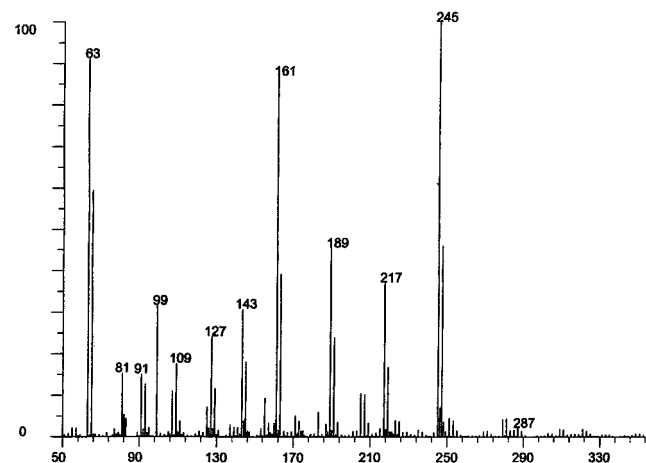
Figure 1. CI-FAB mass spectrum that results from the reaction of Cu$^+$ sputtered from copper foil, with triethyl phosphate.

associated with a stabilizing charge concentration within the bonding region. The AIM analysis was performed using the AIMPAC series of programs.[35]

NBO[36] analysis of Weinhold et al. has also been performed to obtain the natural total charges for the different atoms of each system, as well as a description of the bonding, in terms of the natural atomic orbitals (or hybrids) centered on atoms of particular interest.

Results and Discussion

Figure 1 shows the CI-FAB mass spectrum that results from the gas-phase reactions of Cu$^+$ ions with triethyl phosphate. The existence of ^{63}Cu and ^{65}Cu isotopes leads to an easy
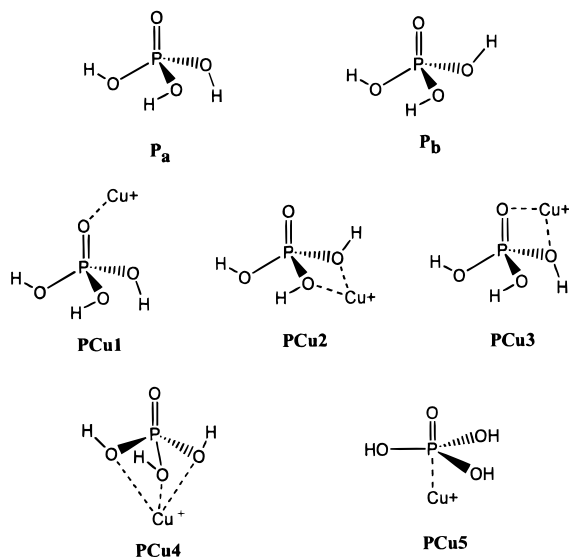
SCHEME 1
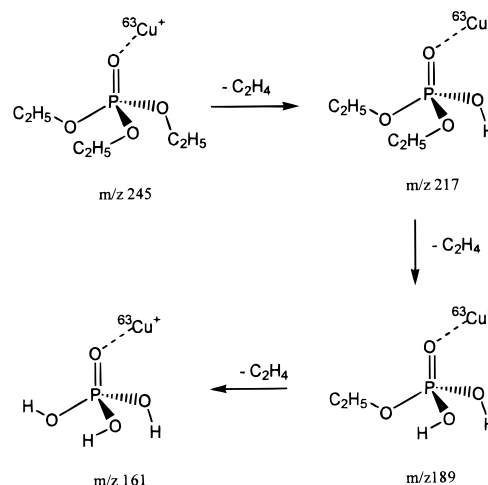
identification of copper-containing ions. We can remark that if these two ions are produced in a ratio that is close to that of their natural abundance (69/31), the adduct ions containing the ^{63}Cu isotope are always more abundant. In this spectrum, besides the metallic Cu$^+$ ions at *m/z* 63 and 65 and copper clusters Cu$_2$H$^+$ ions at *m/z* 127, 129, and 131 several copper/organic ions can be observed. The base peak of this spectrum, at *m/z* 245, corresponds to the formation of the triethyl phosphate−^{63}Cu$^+$ adduct ion, which undergoes facile dissociation, by stepwise elimination of C$_2$H$_4$, to form successively diethyl and ethyl phosphate−^{63}Cu$^+$ complexes (at *m/z* 217 and 189, respectively) and an abundant ion at *m/z* 161 corresponding to the orthophosphoric−^{63}Cu$^+$ adduct ion. The intensity of this ion must be related to the high stability of this complex, which motivates the study presented here. Starting from the triethyl phosphate−Cu$^+$ adduct ion, the mechanism displayed in Scheme 1 could be proposed for the generation of the (HO)$_3$P=O−Cu$^+$-complex. The last of the ions containing the copper ion (at *m/z* 143 and 145) are formed by the loss of H$_2$O from the (HO)$_3$P=O−Cu$^+$ complex. The resulting ions could correspond to the metaphosphoric−Cu$^+$ complexes. This reactivity looks like that of the protonated orthophosphoric acid, which we have recently reported.[21b] Moreover, it can be noted that in our CI-FAB chemical ionization conditions, this P(OH)$_4$$^+$ ion at *m/z* 99 is also formed and it loses, as expected, a water molecule, leading to the *m/z* 81 ion. A similar scheme of P(OH)$_4$$^+$ ion production by electron impact ionization of trialkyl phosphates has been reported recently by Tureček.[37]

The gas-phase reactivity of Cu$^+$ with trimethyl phosphate (CH$_3$O)$_3$P=O leads, in the same experimental conditions, to an abundant trimethyphosphate−Cu$^+$ adduct ion. Nevertheless, this complex does not decompose to yield the cationized monomethylphosphoric acid ester (CH$_3$O)(OH)$_2$P=O- - -Cu$^+$. One of the neutral precursors that could lead to the formation of this adduct ion would be the methyl diethyl phosphate. The corresponding Cu$^+$ adduct ions could undergo facile dissociation, by stepwise elimination of C$_2$H$_4$, to form successively methyl ethyl and methyl phosphate−Cu$^+$ complexes. The methyl diethyl phosphate is unfortunately not commercially available and its synthesis is rather tricky. Yet, we can assume that the adduct ion CH$_3$(OH)$_2$P=O- - -Cu$^+$ can be generated in the gas phase and its stability theoretically estimated.

So, the results presented hereafter are focused on the structural and the associate energetics of the adduct ions that can result from the association of Cu$^+$ with orthophosphoric acid and its monomethyl ester.

SCHEME 2

1. [(HO)₃PdO, Cu⁺] Complexes. All the possible direct adducts formed by direct association of orthophosphoric acid with Cu⁺ are presented in Scheme 2, and the geometries of the different minima of neutral and cationized species are shown in Figure 2. The absolute and relative energies of all the complexes considered in this study are listed in Table 1.

We have considered two conformations for the orthophosphoric acid, namely, P_a and P_b, which differ by the cis or trans O—H position (see Scheme 2). The computational results showed that these two conformations are energetically almost degenerate. The first conspicuous fact of the $[H_3, P, O_4, Cu]^+$ hypersurface is that the global minimum PCu1 corresponds to the direct association of Cu⁺ to the oxygen atom of the P=O bond. Here we can mention that such a complexation over the structure Pb evolved without activation barrier to the same complex PCu1, undoubtedly because of the repulsion between the positive charge of Cu⁺ and the hydrogen atom in cis position of the O—H group in the structure Pb.

The metal association to two of the hydroxylic oxygen atoms leads to a minimum PCu2 located at 23.9 kcal/mol above PCu1. Finally, the association of Cu⁺ to the three hydroxylic oxygen atoms of orthophosphoric acid leads to the less stable species, PCu4, where the Cu—O distance is considerably enlarged with respect to that found for the other minima. The frequency calculations revealed PCu4 to be a second-order transition state. The reaction coordinates corresponding to these imaginary frequencies lead to the formation of PCu1.

The optimization procedure over the PCu3 and PCu5 structures did not evolve to stationary points with the structures proposed in Scheme 2. In the case of PCu3, it evolved without activation barrier to any of PCu1 or PCu2, depending on the starting geometry. For PCu5 we considered it as a feasible structure since this is the one found in PCl₅. However, in our case, all the attempts to optimize this species have evolved without activation barrier to the geometry of PCu4. The direct implication of this feature is that any of the oxygen atoms of (HO)₃P=O is more basic than phosphorus atom when the Cu⁺ cation is the reference acid.

Discussion of the Theoretical Method. It is worth mentioning that the B3LYP/LANL2DZ level of theory (see Table 1) predicts a difference of energy of only 7.1 kcal/mol between PCu1 and PCu2. This result shows a great quantitative difference with respect to our augmented all electron basis set (23.9 kcal/mol).

To investigate the origin of this difference, we have performed several calculations with different basis sets of double and triple-ζ quality (see Table 3).

The first conspicuous fact is that geometry optimization at the B3LYP/6-31G level shows an energy gap between PCu1 and PCu2 of only 1.9 kcal/mol. The simple inclusion of one set of 5d and one set of 7f polarization functions on Cu, O, and P atoms increases the difference up to 15.8 kcal/mol. This shows the great importance of polarization functions to describe the energetics of these kinds of systems. So, considering the geometries under consideration, as well as the bond angles typically found at phosphorus, a basis set with a set of d functions is the minimum level for consideration. Hence, it is not surprising to find that the B3LYP/LANL2DZ method underestimates the energy gap since this basis set does not include polarization functions. Furthermore, from Table 3 we also see that the change from the double-ζ 6-31G(d) basis set to the triple-ζ 6-311G(d,p) increases the PCu1—PCu2 energy gap up to 18.6 kcal/mol. Also importantly, Table 3 shows that the greater the number of polarization functions, the greater the energy difference between our global and second minima of the hypersurface, which converges at the highest level to a value of 22.3 kcal/mol. This value is very similar to that found when B3LYP/LANL2DZ optimized geometry is used (i.e., 23.9 kcal/mol). In addition, the calculations at B3LYP/Base1//B3LYP/6-311G(d,p) have been tested and demonstrated to be reliable enough through comparison with G2 tests.[27a]

Binding Properties. In Table 4 we can find the natural charges obtained in the NBO analysis as well as the topological analysis used to investigate the nature of the Cu—O bonds and the possible activations upon complexation. We can see that the elongation of the P—O bonds contiguous to its association accompanies the Cu⁺ complexation. This effect has been widely observed and explained the differences of electronegativities between the phosphorus and oxygen atoms; since oxygen is a very electronegative atom, it recovers part of the charge transferred to Cu⁺ by depopulating the other P—O bonds. The opposite effect is observed for the remaining P—O bonds. Those bonds that do not suffer the Cu⁺ association directly are reinforced by the effect of the increase of P⁺O⁻ polarization induced by the greater electronegativity of the oxygen atom. This is in agreement with the observed change of stretching frequencies upon complexation. In neutral phosphoric acid, the three P—OH stretchings have the values 682, 765, and 784 cm⁻¹, while these values are blue shifted in complex PCu1 to 708, 770, and 799 cm⁻¹, respectively. On the contrary, the P=O stretching of 1131 cm⁻¹ in neutral H_3PO_4 is red shifted down to 1098 cm⁻¹ upon complexation in PCu1 complex.

We can observe that the electronic density (ρ) of the CuO bonds is bigger than those corresponding to almost pure electrostatic bonds. In previous studies, i.e., in formamide—Li⁺ and formamide—Na⁺ [10a] reactions, we found that the values of the electronic densities for O—Li⁺ and O—Na⁺ bonds were 0.038 and 0.028 e/au³, respectively. The fact that O—Cu⁺ densities at least duplicate these values prompts us to think that some covalent character exists in this case. This is corroborated by the values of the energy densities $H(r)$ at the bond critical points, which are all negatives, but at least 1 order of magnitude greater than those found for PO and OH bonds, where a dominant covalent character is expected. Some other previous studies[27a] from Cu—N bonds where the degree of hybridization of N was ranging from sp to sp³ showed densities in the interval 0.115—0.125 e/au³. Therefore, we can conclude that we have
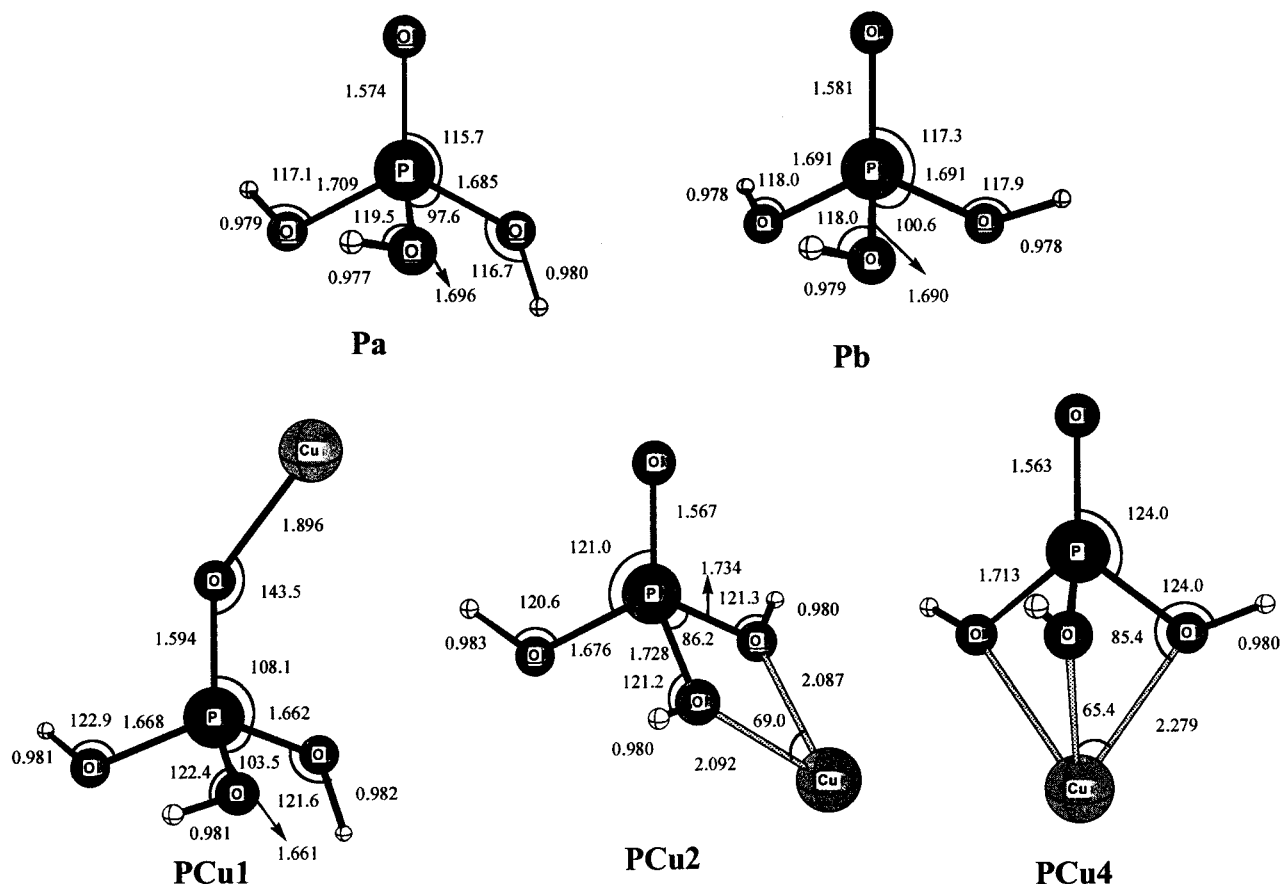
Figure 2. B3LYP/LANL2DZ optimized geometries of the different stationary points corresponding to [(OH)₃P=O, Cu⁺] complexes. Bond lengths are in Å, and angles, in degrees.

TABLE 3: Absolute Energies (Hartrees), Relative Energies Including ZPE (kcal/mol) of P$_a$, P$_b$, PCu1, and PCu2 Species

basis set	PCu1	PCu2	P$_a$	P$_b$	ΔE^c
6-31G	−2283.902205	−2283.899231			1.9[a]
6-31G(d)	−2284.145123	−2284.119967			15.8[a]
ZPE 6-311G(d,p)	0.049917	0.050194	0.048620	0.048641	
6-311G(d,p)	−2284.474776	−2284.445427	−644.2677549	−644.2691588	18.6
6-311G(2d,2p)[b]	−2284.511920	−2284.481141	−644.3045458	−644.3063315	19.5
6-311G(2df,2p)[b]	−2284.532711	−2284.499758	−644.3229332	−644.3247504	20.9
6-311+G(2df,2p)[b]	−2284.608224	−2284.572916	−644.3347795	−644.3363923	22.3

[a] These values does not include ZPE correction. [b] These values correspond to single point calculations over the 6-311G(d,p) optimized geometry. [c] Relative energy between PCu1 and PCu2.

TABLE 4: Evaluation at the Corresponding Bond Critical Point of Charge Densities (ρ), Laplacian of the Charge Densities ($\nabla^2\rho$), and Energy Densities ($H(r)$)

	P			PCu1			PCu2		
	ρ	$\nabla^2\rho$	$H(r)$	ρ	$\nabla^2\rho$	$H(r)$	ρ	$\nabla^2\rho$	$H(r)$
Cu—O				0.092	0.550	−0.013	0.062	0.308	−0.010
O=P	0.201	0.736	−0.167	0.188	0.681	−0.150	0.203	0.768	−0.168
P—O	0.154[b]	0.308[b]	−0.121[b]	0.164[b]	0.410[b]	−0.129[b]	0.142[b] (0.161)	0.223[b] (0.360)	−0.111[b] (−0.127)
charge Cu					0.914			0.964	
charge O P=O		−0.971			−1.141			−0.889	
charge O P—O		−0.965[b]			−0.951[b]			−1.048[b] (−0.943)	
charge P		2.346			2.464			2.328	

[a] Natural charges were evaluated from a NBO analysis. Values between parentheses correspond to the non-Cu⁺-complexed O—H. All values are in au. [b] These values correspond to the averaged values between the several quasi-equivalent P—OH bonds.

an intermediate situation, which prompted us to further explore the nature of the Cu—O bonds.

The values of the Cu⁺ natural charges reveal that the interaction of Cu⁺ with O is essentially electrostatic, although there exists a nonnegligible covalent character, which we can explain as follows: in the case of PCu1 only 0.086 e⁻ is transferred to oxygen; for PCu2 the charge transferred is even lower, only 0.036. This fact is in agreement with the greater degree of covalence observed in the O—Cu bond in the PCu1 system, reflected in the value of its electronic density in the bond critical point. More interestingly, while in PCu2 the NBO analysis failed to locate any of the Cu—O bonds, in PCu1 such analysis located a Cu—O bond, which can be seen as a dative bond where a hybrid sp with a strong p character of the oxygen
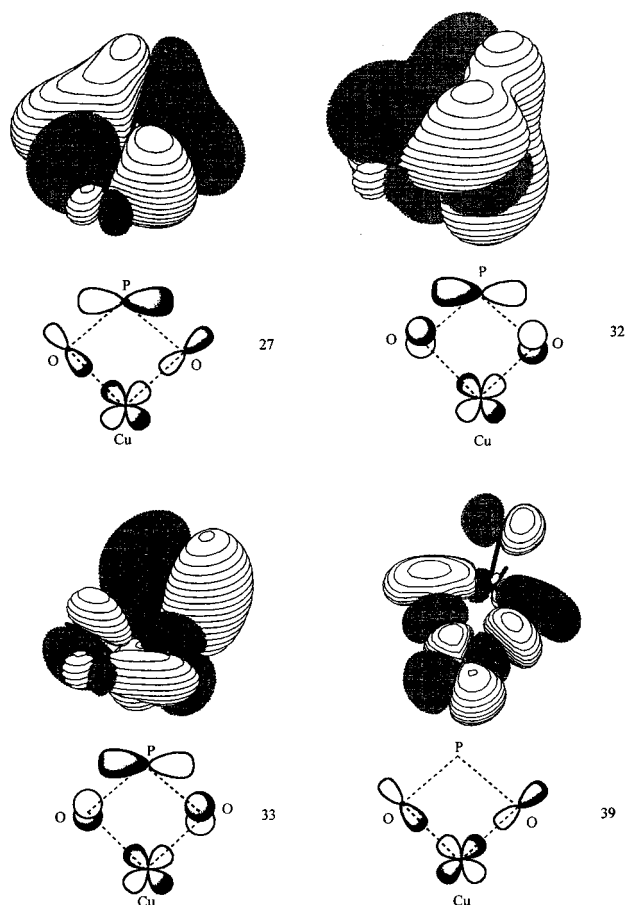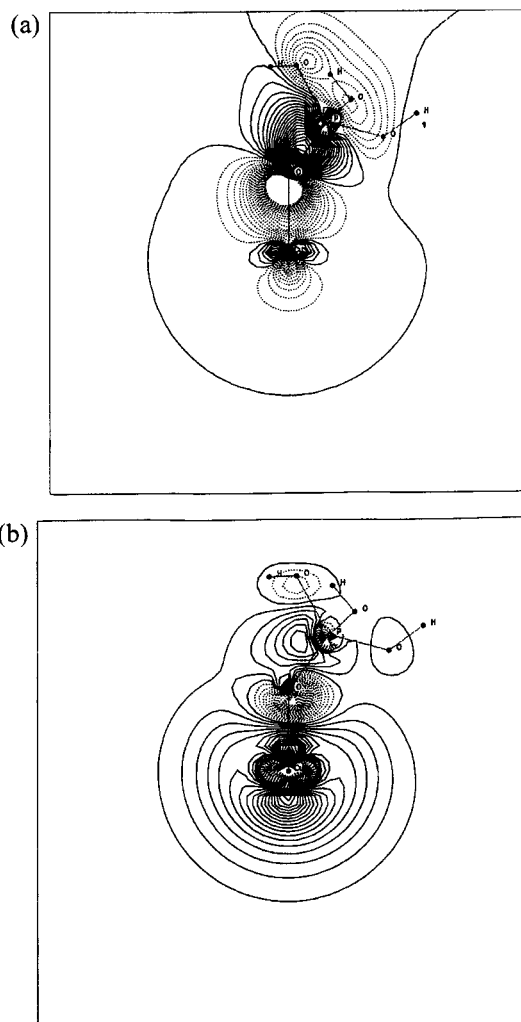
Figure 3. Diagram of the molecular orbitals associated with the bonding of Cu to the P(OH)$_2$ bonds, in PCu2 complexes.

has 95.9% participation. The contribution of Cu$^+$ is made by means of an sd hybrid with a strong character of 87.2% s character.

This difference in the features of the location of Cu—O bonds can be explained by an analysis of its canonical orbitals. In PCu2, the only orbital that has some relevant contributions in the internuclear O—Cu—O area is the d$_{x^2-y^2}$ atomic orbital of copper in the 39 doubly occupied molecular orbitals. We can see in Figure 3 the four having a significant participation of the aforementioned d$_{x^2-y^2}$ orbital. The 32 and 33 molecular orbitals do not possess a good overlap of d$_{x^2-y^2}$ orbital of the copper with out-of-plane p orbitals of the oxygen atom. Therefore, these orbitals cannot be considered responsible for an effective covalent interaction. On the contrary, the molecular orbital 27 exhibits a strong overlap among the aforementioned orbitals, which confers a bonding character. However, the strong antibonding character of the doubly occupied (HOMO) orbital 39 counteracts this effect. This cancelation of effects makes the localization of the bonds difficult.

The effect is different in PCu1: we observe that in Figure 4 the orbital corresponding to the bonding character for P=O- - -Cu bond. This orbital has a great participation of the hybrid sp of the oxygen, which has a great p character. The corresponding antibonding Cu—O orbital having an effective overlap between atomic orbitals of Cu and O is the unoccupied LUMO orbital 40, contrary to what happened in PCu2 system.

2. [(CH$_3$ O)(HO)$_2$P=O, Cu$^+$] Complexes. As stated in the Introduction, we considered the monomethylated forms of orthophosphoric acid in order to approach more accurately the model that will be found in nucleotides.


Figure 4. Contour map of the molecular orbitals associated with the bonding of Cu to the P=O bond in PCu1 complexes.

SCHEME 3
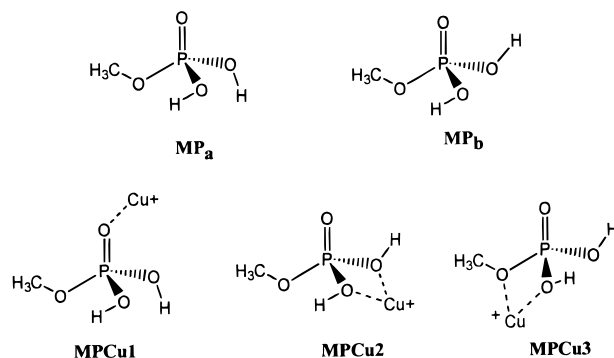
From a theoretical point of view, all the possible sites of cationization have been envisaged (see Scheme 3) by disregarding those structures, which would correspond to monomethylated PCu3 and PCu5 in Scheme 2. We can see the geometries of the corresponding neutral and cationized minima in Figure 5. The neutral MP$_a$ and MP$_b$ are also very close in energy. As could be have expected, there is no significant difference between the geometrical parameters in PCu1 and MPCu1. The same trends are observed for PCu2 and MPCu2, MPCu3 species. In these last systems where Cu is bisligated to two oxygen atoms, the structure MPCu2 is slightly more stable (2 kcal/mol)
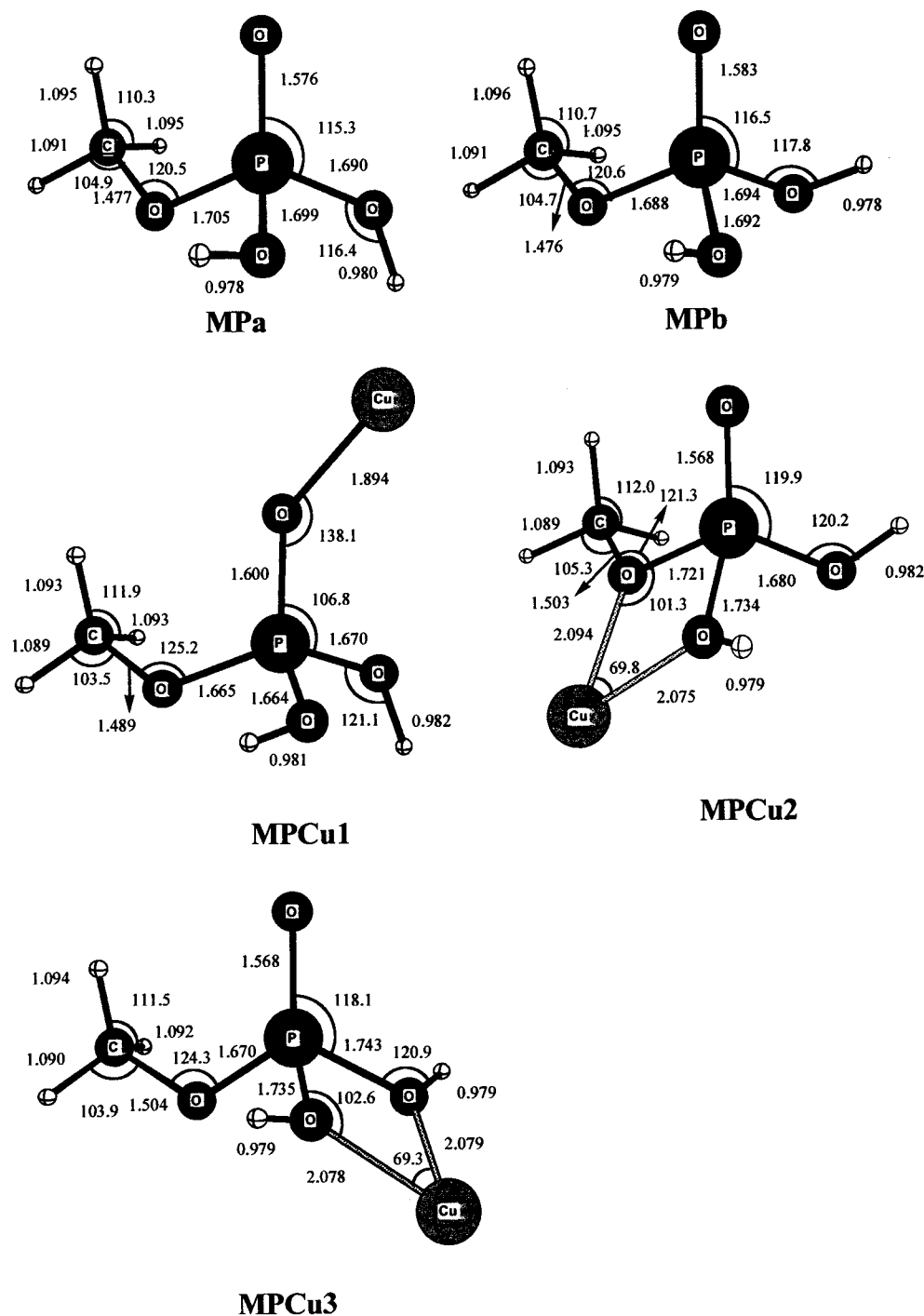
Figure 5. B3LYP/LANL2DZ optimized geometries of the different stationary points corresponding to [(OCH$_3$)(OH)$_2$P=O, Cu$^+$] complexes. Bond lengths are in Å, and angles, in degrees.

than MPCu3 because of the inductive effect of the methyl group to the oxygen that directly participates in the essentially ionic bond.

We can observe that, for methylated species, the structural features of P—OH bonds are similar to those found for orthophosphoric acid: complexation of MPa to species MPCu1 gives rise to the elongation of the P=O bond, while the P—OH contiguous ones are slightly reinforced. The complexation of MPb to MPCu3 and MPCu2 has the same effect: P—OH and OCH$_3$ bonds that are directly affected are elongated and the P=O bond is slightly reinforced.

3. Binding Energies. As we can see in Table 1, using B3LYP/LANL2DZ optimized geometries, the calculated binding energy of orthophosphoric acid to Cu$^+$ is about 61 kcal/mol

when the cationization site is the phosphonate oxygen atom (P= O). The value obtained by optimizing with an all-electrons basis set is 58.9 kcal/mol (see Table 5); this corroborates the compromise of feasibility/reliability of the use of the LANL2DZ pseudopotential. The effect of the methyl group is just to increase only slightly these values in ca. 2 kcal/mol. When the cationization is performed via the double-liganded complex, the covalent contribution is minimized in order to have more electrostatic interaction, and then the binding energies are reduced to 40 kcal/mol. Again, the methylation induces a slight increase in the binding energies.

As stated in previous works, the binding energies for Cu$^+$ association with formamide[5] and guanidine[4] are 56.2 and 77.9 kcal/mol, respectively. We can consider these systems as

Phosphate Group Interaction with Gas-Phase Cu(I)

J. Phys. Chem. B, Vol. 104, No. 1, 2000 **117**

TABLE 5: Binding Energy Including ZPE (kcal/mol) of PCu1 Species Evaluated with Different "All Electron" Basis Sets

basis set	binding energy of PCu1
B3LYP/6-311G(d,p)	64.2
B3LYP/6-311G(2d,2p)[b]	64.2
B3LYP/6-311G(2df,2p)[b]	65.7
B3LYP/Base1//B3LYP/6-311G(d,p)	58.9

[b] These values correspond to single point calculations over the 6-311G(d,p) optimized geometry.

moieties present on the nucleobases. More interesting, the Cu^+ binding energies for guanine and adenine are expected to be of the same order if we refer to the values previously reported by Burda et al.[38] By using the MP2/pseudopotential, these authors estimated the Cu^+ binding energies for guanine and adenine to be 56.6 and 80.3 kcal/mol, respectively.

Thus, from these aforementioned estimated values we can deduce that, at least in the case of guanosine monophosphate, the complexation could give rise to some structures in which the Cu^+ ion would interact with the two subunits, the neutral phosphate group and the guanine moiety.

Conclusions

Experimentally, the reaction of triethyl phosphate with $^{63}Cu^+$ in FAB conditions produces abundant ions at $m/z = 161$ corresponding to the adduct of Cu^+ with the orthophosphoric acid $(HO)_3P=O$. As phosphoric acid seems to be a good model to represent neutral phosphate features in nucleotides, we have studied the possible complexations of Cu^+ to the different basic centers in this system. We have found that the O—Cu bonds are essentially electrostatic, but they present a nonnegligible covalent character, which makes more feasible the interaction of Cu^+ with the P=O oxygen group than with two or three hydroxyl groups at the same time, where the covalent interaction would be inferior. We have localized the molecular orbitals responsible for the covalent contributions in O—Cu^+ bonds. The possibility of activation of the several P—O bonds upon complexation with Cu^+ has also been shown. We have observed by means of a topological analysis that such an elongation is produced in the P—O bond directly involved in the complexation, while reinforcement of the other P—O bonds is the consequence of the difference of electronegativities between P and O. Methylation does not change this behavior.

The binding energies for Cu^+ association with orthophosphoric acid and its monomethylated ester have also been evaluated to be 61.1 and 63.2 kcal/mol, respectively, at the B3LYP/Base1//B3LYP/LAN2DZ level, when the cationization site is the phosphate oxygen atom (P=O). For orthophosphoric acid the value obtained by optimizing the geometry with an "all-electrons" basis set is 58.9 kcal/mol (see Table 2); this corroborates the compromise of feasibility/reliability of the use of ECPs with the valence basis set LANL2DZ for geometry optimizations. These Cu^+ binding energy values, compared with the available published data for the natural nucleobases guanine and adenine, suggest that a competition between the neutral phosphate group and the basic centers present in guanine would take place in the gas phase, to accommodate at best the monocation Cu^+.

References and Notes

(1) (a) *Organometallic Ion Chemistry*; Freiser, B. S., Ed.; Kluwer Academic Publishers: Dordrecht, The Netherlands, 1996. (b) Armentrout, P. B.; Baer, T. *J. Phys. Chem. A* **1996**, *100*, 12866 and references therein. (c) Eller, K.; Schwarz, H. *Chem. Rev.* **1991**, *91*, 1121. (d) Eller, K. *Coord. Chem. Rev.* **1993**, *126*, 93.

(2) (a) Grese, R. P.; Cerny, R. L.; Gross, M. L. *J. Am. Chem. Soc.* **1989**, *111*, 2835. (b) Hu, P.; Gross, M. L. *J. Am. Chem. Soc.* **1993**, *115*, 8821. (c) Reiter, A.; Adams, J.; Zhao, H. *J. Am. Chem. Soc.* **1994**, *116*, 7827. (d) Ma, S.; Wong, P.; Yang, S. S.; Cooks, R. G. *J. Am. Chem. Soc.* **1996**, *118*, 6010. (e) More, M. B.; Ray, D.; Armentrout, P. B. *J. Phys. Chem. A* **1997**, *101*, 7007. (f) Lee, S.; Kim, H. S.; Beauchamp, J. L. *J. Am. Chem. Soc.* **1998**, *120*, 3188. (g) Cerda, B. A.; Wesdemiotis, C. *J. Am. Chem. Soc.* **1996**, *118*, 11884. (h) Gatlin, C. L.; Tureček, F.; Vaisar, T. *J. Am. Chem. Soc.* **1995**, *117*, 3637.

(3) (a) Hoyau, S.; Ohanessian, G. *J. Am. Chem. Soc.* **1997**, *119*, 2016. (b) Sponer, J.; Burda, J. V.; Sabat, M.; Leszczynski, J.; Hobza, P. *J. Phys. Chem. A* **1998**, *102*, 5997.

(4) Luna, A.; Amekraz, B.; Morizur, J.-P.; Tortajada, J.; Mó, O.; Yáñez, M. *J. Phys. Chem. A* **1997**, *101*, 5931.

(5) Luna, A.; Amekraz, B.; Tortajada, J.; Morizur, J.-P.; Alcamí, M.; Mó, O.; Yáñez, M. *J. Am. Chem. Soc.* **1998**, *120*, 5411.

(6) Luna, A.; Morizur, J.-P.; Tortajada, J.; Alcamí, M.; Mó, O.; Yáñez, M. *J. Phys. Chem. A* **1998**, *102*, 4652.

(7) Alcamí, M.; Mó, O.; Yáñez, M.; Luna, A.; Morizur, J.-P.; Tortajada, J. *J. Phys. Chem. A* **1998**, *102*, 10120.

(8) Luna, A.; Amekraz, B.; Tortajada, J.; Morizur, J.-P.; Mó, O.; Yáñez, M. Submitted for publication.

(9) (a) Cerda, B. A.; Wesdemiotis, C. *J. Am. Chem. Soc.* **1995**, *117*, 9734. (b) Wen, D.; Yalcin, T.; Harrison, A. G. *Rapid Commun. Mass Spectrom.* **1995**, *9*, 1155. (c) Bouchonnet, S.; Hoppilliard, Y.; Ohanessian, G. *J. Mass. Spectrom.* **1995**, *30*, 172. (d) Lavanant, H.; Hoppilliard, Y. *J. Mass. Spectrom.* **1997**, *32*, 1037. (e) Speir, J. P.; Gorman, G. S.; Amster, I. J. *J. Am. Soc. Mass. Spectrom.* **1993**, *4*, 106. (f) Lei, Q. P.; Amster, I. J. *J. Am. Soc. Mass Spectrom.* **1996**, *7*, 722.

(10) (a) Tortajada, J.; Leon, E.; Morizur, J.-P.; Luna, A.; Mó, O.; Yáñez, M. *J. Phys. Chem.* **1995**, *99*, 13890. (b) Amekraz, B.; Tortajada, J.; Morizur, J. P.; González, A. I.; Mó, O.; Yáñez, M. *THEOCHEM* **1996**, *371*, 313. (c) Leon, E.; Amekraz, B.; Tortajada, J.; Morizur, J.-P.; González, A. I.; Mó, O.; Yáñez, M. *J. Phys. Chem. A* **1997**, *101*, 2489.

(11) Jones, R. W.; Staley, R. H *J. Am. Chem. Soc.* **1982**, *104*, 2296.

(12) Murray, K. K. *J. Mass Spectrom.* **1996**, *31*, 1203.

(13) Crain, P. F. *Mass Spectrom. Rev.* **1990**, *9*, 505.

(14) Fenn, J. B.; Mann, M.; Meng, C. K.; Wong, S. F.; Whitehouse, C. M. *Mass Spectrom. Rev.* **1990**, *9*, 37.

(15) Hillenkamp, F.; Karas, M.; Beavis, R. C.; Chait, B. T. *Anal. Chem.* **1991**, *63*, 1193A.

(16) (a) Stemmler, E. A.; Hettich, R. L.; Hurst, G. B.; Buchanam, M. V. *Rapid Commun. Mass Spectrom.* **1993**, *7*, 828 (b) Stemmler, E. A.; Buchanam, M. V.; Hurst, G. B.; Hettich, R. L. *Anal. Chem.* **1995**, *67*, 2924.

(17) Gut, I.; Beck, S. *Nucl. Acids Res.* **1995**, *23*, 1367.

(18) Pieles, U.; Zürcher, W.; Schär, M.; Moser, H. E. *Nucl. Acids Res.* **1993**, *21*, 3191.

(19) (a) *The chemistry of organophosphorus Compounds*; O'Hair, R. A. J., Ed.; Wiley: Chichester, U.K., 1996, Vol. 4, p 731. (b) Van Wazer, J. R.; Ewig, C. S. *J. Am. Chem. Soc.* **1985**, *107*, 1965; **1986**, *108*, 4354. (c) George, L.; Viswanathan, K. S.; Singh, J. *J. Phys. Chem. A* **1997**, *101*, 2459.

(20) Morris, R. A.; Knighton, W. B.; Viggiano, A. A.; Hoffman, B. C.; Schaefer, H. F. *J. Chem. Phys.* **1997**, *106*, 3545.

(21) (a) Tureček, F.; Gu, M.; Hop, C. E. C. A. *J. Phys. Chem.* **1995**, *99*, 2278. (b) Gevrey, S.; Luna, A.; Haldys, V.; Tortajada, J.; Morizur, J.-P. *J. Chem. Phys.* **1998**, *108*, 2458.

(22) Harrison, A. G.; Mercer, R. S.; Reiner, E. J.; Young, A. B.; Boyd, R. K.; March, R. E.; Porter, C. J. *Int. J. Mass Spectrom. Ion Processes* **1986**, *74*, 13.

(23) (a) Freas, R. B.; Ross, M. M.; Campana, J. E. *J. Am. Chem. Soc.* **1985**, *107*, 6195. (b) Freas, R. B.; Campana, J. E. *J. Am. Chem. Soc.* **1985**, *107*, 6202.

(24) (a) Drewello, T.; Eckart, K.; Lebrilla, C. B.; Schwarz, H. *Int. J. Mass Spectrom. Ion Processes* **1987**, *76*, 13. (b) Hornung, G.; Schröder, D.; Schwarz, H. *J. Am. Chem. Soc.* **1995**, *117*, 8192.

(25) (a) Becke, A. D. *J. Chem. Phys.* **1993**, *98*, 5648. (b) Becke, A. D. *J. Chem. Phys.* **1992**, *96*, 2155.

(26) Gaussian 94, Frisch, M. J.; Trucks, G. W.; Schlegel, H. B.; Gill, P: M.W.; Johnson, B. G.; Robb, M. A.; Cheeseman, J. R.; Keith, T. A.; Peterson, G. A.; Montgomery, J. A.; Raghavachari, K.; Al-Laham, M. A.; Zakrzewski, V. G.; Ortiz, J. V.; Foresman, J. B.; Croslowski, J.; Stefanow, B. B.; Nanayakkara, A.; Challacombe, M.; Peng, C. Y.; Ayala, P. Y.; Chen, W.; Wong, M. W.; Andres, J. L.; Replogle, E. S.; Gomperts, R.; Martin, R. L.; Fox, D. J.; Binkley, J. S.; Defrees, D. J.; Baker, J.; Stewart, J. P.;

Head-Gordon, M.; Gonzalez, C.; Pople, J. A. *Gaussian94*; Gaussian, Inc. Pittsburgh, PA, 1995.

(27) (a) Luna, A.; Amekraz, B.; Tortajada, J. *Chem. Phys. Lett.* **1997**, *266*, 31. (b) Hoyau, S.; Ohanessian, G. *Chem. Phys. Lett.* **1997**, *280*, 266. (c) Bauschlicher, C.; Ricca, A.; Partridge, H.; Langhoff, S. R. In *Recent Advances in Density Functional Theory*; Chong, D. P., Ed.; World Scientific Publishing Co.: Singapore, 1997; Part II.

(28) Lee, C.; Yang, W.; Parr, R. G. *Phys Rev.* **1988**, *B37*, 785.

(29) (a) Hay, P. J.; Wadt, W. R. *J. Chem. Phys*. **1985**, *82*, 270. (b) Wadt, W. R; Hay, P. J. *J. Chem. Phys*. **1985**, *82*, 284. (c) Hay, P. J.; Wadt, W. R. *J. Chem. Phys*. **1985**, *82*, 299.

(30) (a) Dunning, T. H. *J. Chem. Phys.* **1970**, *52*, 2823. (b) Huzinaga, S. *J. Chem. Phys.* **1965**, *42*, 1293.

(31) (a) Wachters, A. J. H. *J. Chem. Phys.* **1970**, *52*, 1033. (b) Hay, P. J. *J. Chem. Phys.* **1977**, *66*, 4377.

(32) Rassolov, V.; Pople, J. A.; Ratner, M.; Windus, T. L. *J. Chem. Phys.* **1998**, *109*, 1223.

(33) Bader, R. F. W. *Atoms in Molecules. A Quantum Theory;* Oxford University Press: Oxford, U.K., 1990.

(34) (a) Cremer, D.; Kraka, E. *Croat. Chim. Acta* **1984**, *57*, 1529. (b) Cremer, D.; Kraka, E. *Angew. Chem., Int. Ed. Engl.* **1984**, *23,* 627.

(35) The AIMPAC programs package has been provided by J. Cheeseman and R. F. W. Bader.

(36) *The Structures of Small Molecules and Ions*; Weinhold, F., Carpenter, J. E., Eds.; Plenum Press: New York, 1988.

(37) Turecek, F. *Int. J. Mass Spectrom.* **1998**, *33*, 779.

(38) Burda, J. V.; Šponer, J.; Hobza, P. *J. Phys. Chem*. **1996**, *100*, 7250.